CHEMISTRY
A EUROPEAN JOURNAL

DOI: 10.1002/chem.200901392

Iron-Substituted Polyoxotungstates as Inorganic Synzymes: Evidence for a Biomimetic Pathway in the Catalytic Oxygenation of Catechols

Andrea Sartorel,[b] Mauro Carraro,[b] Gianfranco Scorrano,[b] Bassem S. Bassil,[a] Michael H. Dickman,[a] Bineta Keita,[c] Louis Nadjo,[c] Ulrich Kortz,*[a] and Marcella Bonchio*[b]

Dedicated to the Centenary of the Italian Chemical Society

The oxygenase activity of natural metallo-enzymes offers a unique paradigm of what is the Holy Grail of oxidation chemistry.[1–4] An innovative approach to the design of oxygenase functional mimics is the adoption of a totally inorganic ligand system derived from polyoxometalates (POMs),[5–7] as an alternative to organic or organometallic coordination complexes.[8–9] Bio-inspired activity of transition-metal-substituted POMs (TMSP, with TM being Fe, Mn, Ru) has been proposed in the recent literature.[10–14] However, due to the severe mechanistic complexity, which is frequently associated with metal-mediated aerobic oxidations, it is a major challenge to unravel the catalyst's role along oxygen-transfer pathways. Therefore, in the realm of POM-based oxygenase mimics, the adherence to bio-inspired mechanistic features is often a matter of debate and retains a fundamental interest.[15,16] Among the class of Fe-substituted polyoxotungstates some structural types are known, where the coordination geometry of the iron center exhibits a striking oxygenase synzyme motif (Figure S1).[17] In particular, the tetrasubstituted Krebs-type polyanions with general formula $[Fe_4(H_2O)_{10}(\beta\text{-}XW_9O_{33})_2]^{n-}$ ($Fe_4X_2W_{18}$, $X=As^{III}$, Sb^{III}; $n=6$; $X=Se^{IV}$, Te^{IV}; $n=4$), display two of the four iron sites with three terminal, substitution-labile coordination positions, typical of non-heme dioxygenase enzymes (Figure 1).[18] The latter are responsible for the catabolism/biodegradation of dihydroxylated aromatic compounds. While several functional models have been designed with coordination complexes using polydentate organic ligands,[8] very few examples deal with POM-based systems, and Fe^{III} framework-incorporated POMs as multi-turnover catalysts for the aerobic cleavage of catechols are unprecedented.[19]

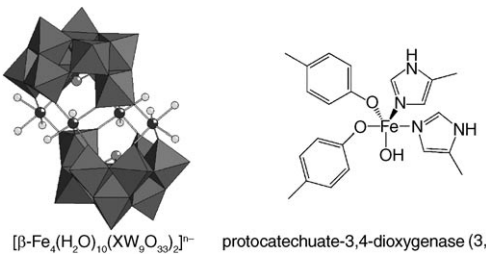

Figure 1. Structure of a Krebs-type Fe-substituted polyoxotungstate (left) and of the active site coordination geometry of protocatechuate-3,4-dioxygenase (right).

Herein we report combined and convergent structural, spectroscopic and mechanistic evidence on the bio-inspired catalysis by Krebs-type $Fe_4X_2W_{18}$ polytungstates in promoting the cleavage of catechols. The biomimetic function of the POM-based catalyst is assessed by spectroscopic and structure–reactivity relationships. According to the generally accepted hypothesis (Scheme 1), the initial steps of the enzymatic mechanism involve catechol deprotonation and its chelation to the Fe center (a–b in Scheme 1).[8,20] The Fe^{III}–catecholate intermediate displays a Fe^{II}–semiquinonate char-

[a] Dr. B. S. Bassil, Dr. M. H. Dickman, Prof. U. Kortz
School of Engineering and Science
Jacobs University P.O. Box 750 561, 28725 Bremen (Germany)
Fax: (+49) 421-200-3229
E-mail: u.kortz@jacobs-university.de

[b] Dr. A. Sartorel, Dr. M. Carraro, Prof. G. Scorrano, Dr. M. Bonchio
ITM-CNR and Department of Chemical Science
University of Padova, via Marzolo 1, 35131 Padova (Italy)
Fax: (+39) 0498275239
E-mail: marcella.bonchio@unipd.it

[c] Dr. B. Keita, Prof. L. Nadjo
CNRS, Equipe d'Electrochimie et Photoélectrochimie
Université Paris-Sud, Bâtiment 350, 91405 Orsay Cedex (France)

Supporting information for this article is available on the WWW under http://dx.doi.org/10.1002/chem.200901392.

acter vis-à-vis ligand-to-metal charge transfer interactions (b and c in Scheme 1). This is the turning point of catalysis, being responsible for substrate activation towards O_2 electrophilic attack (d in Scheme 1). Then, cleavage products are generated from the rearrangement and hydrolysis of a transient alkylperoxo intermediate (e–g in Scheme 1). Milestone results supporting this scenario are provided by mechanistic studies involving mononuclear Fe^{III} complexes and polydentate ligands mimicking the coordination geometry, spectroscopy and function of the natural enzyme.[8,21] 3,5-Di-*tert*-butylcatechol (DTBC) is generally used as the substrate analogue, due to its favorable electron-donating character and stability of the related cleavage products. The biomimetic Fe^{III}–catecholate intermediates have shown some key spectroscopic features, specifically: i) two catecholate-to-Fe^{III} charge transfer bands in the UV/Vis-NIR spectra; ii) the dependence of the complex's reactivity on the energy of such LMCT transitions, as a function of the Lewis acidity of the iron center.

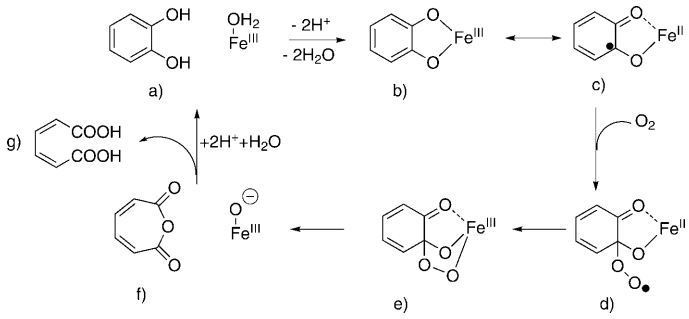

Scheme 1. Biomimetic mechanism for intra-diol cleavage of catechol by Fe^{III} complexes. Spectator ligands on the iron centre are omitted for clarity.

Indeed, red-shifted LMCT transition maxima are associated with a favorable donor–acceptor interaction, thus enhancing the semiquinone character of the bound catecholate, and its reactivity with dioxygen.[22] Following these arguments, the biomimetic potential of the $Fe_4X_2W_{18}$ complexes has been initially screened for DTBC binding, in a weakly coordinating solvent such as 1,2-dichloroethane (DCE), and in protic media such as wet THF and ethanol (Table 1).

Table 1. UV/Vis characterization of $Fe_4X_2W_{18}$/DBTC complexes at 25 °C.

Fe–POM	λ_{max} [nm] (ε [$M^{-1}cm^{-1}$]) (THF/H_2O)	(DCE)	(EtOH)
$Fe_4Te_2W_{18}$	632, (sh, 450), 698 (520)	618 (sh, 1600) 743 (2700)	715 (>2000)
$Fe_4Sb_2W_{18}$	594 (490), 703 (440)	624 (sh, 2600) 729 (3400)	715 (>2000)
$Fe_4As_2W_{18}$	665 (550)	623 (sh, 2100) 714 (2400)	726 (>3000)
$Fe_4Se_2W_{18}$	574 (176)	626 (sh 1800) 706 (1900)	714 (>1000)

In all cases, the formation of a POM–catecholate complex can be monitored by visible spectroscopy, through an increase of the broad absorption bands in the region 570–750 nm (Table 1). Titration profiles with binding saturation are generally observed. Noteworthy, the solvent effect (solvatochromism) on such visible λ_{max} follows the expected trend observed for LMCT transitions, whereby less polar, aprotic solvents give rise to more pronounced red-shifted bands (Table 1).[23] Moreover, the inorganic POM ligand remarkably influences the Fe^{III}–catechol interaction, resulting in diverse λ_{max} values (Table 1).[24,25] The energies of the catecholate-to-Fe^{III} charge-transfer transitions can therefore be tuned by the POM composition. As pointed out above, these bands provide a sensitive probe for the Lewis acidity of the iron center, depending on the donor properties of the ligand set within its coordination sphere. A key aspect is to address the electronic character of the POM moiety by comparing the new observations with the well established database available for classical polydentate organic ligands. In particular, a most informative study has been realized with tetradentate tripod ligands, of general formula $N(CH_2X)_3$, where X is a phenolate, carboxylate, pyridine or benzimidazole functionality (Scheme 2).[22,26,27] Table 1 sheds light on the ligand effect induced by the POM framework. The Lewis acidity of the Fe substituent is not substantially quenched by the overall negative charge of the polyanion. The latter (-4 for $Fe_4Se_2W_{18}$ and $Fe_4Te_2W_{18}$, and -6 for $Fe_4As_2W_{18}$ and $Fe_4Sb_2W_{18}$) is largely associated with the XO_3 hetero groups with some delocalization over the tungsten–oxo framework. Indeed, for $Fe_4X_2W_{18}$, in EtOH as solvent, the LMCT band falls at $\lambda_{max} > 700$, that is, at lower energy compared to a tricarboxylate-based ligand while approaching a mixed ligand set, incorporating two carboxylates and one pendant pyridine (Scheme 2).[22,26]

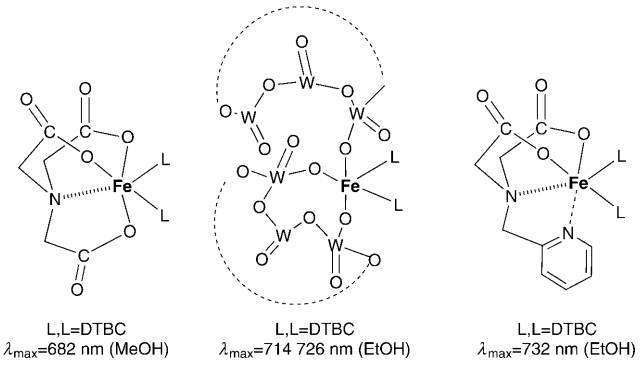

Scheme 2. Comparison of the inorganic POM ligand (middle) with organic tetradentate, tripod-type $N(CH_2X)_3$ ligands (left and right), influencing the spectroscopic properties of Fe–catecholate complexes.

It is noteworthy that the LMCT band red-shifts significantly in the sequence $Fe_4Se_2W_{18} < Fe_4As_2W_{18} < Fe_4Sb_2W_{18} < Fe_4Te_2W_{18}$.

Direct evidence of the substrate-binding mode is provided by the solid-state structures of discrete tetra-oxalato deriva-

tives of $Fe_4X_2W_{18}$ (see Figure 2). We have prepared three oxalato derivatives, namely $[Fe_4(C_2O_4)_4(H_2O)_2(\beta\text{-}XW_9O_{33})_2]^{14-}$ (Ox_4-$Fe_4X_2W_{18}$; X = As^{III}, Sb^{III}, Bi^{III}) by reaction of $Fe_4X_2W_{18}$ (As^{III}, Sb^{III}, Bi^{III}) with $Na_2C_2O_4$ in aqueous acidic medium at pH 4.[28] Recently Dolbecq et al. reported on the structure of the oxalate–antimony derivative Ox_4-$Fe_4Sb_2W_{18}$.[29] Oxalate can be considered as an unreactive analogue of DTBC, coordinating the embedded Fe^{III} centers in a bidentate fashion via two oxygens.[29] Interestingly, the Fe–$O_{oxalate}$ distances resemble those found for some representative Fe–catecholate complexes, in both abiotic and enzymatic systems (Table S4).

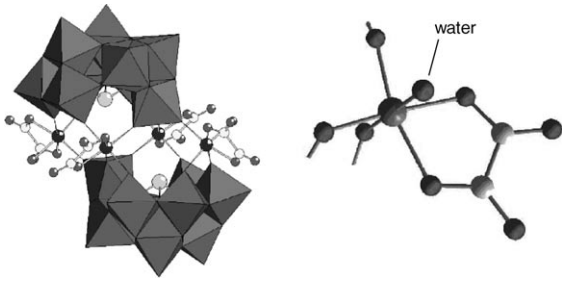

Figure 2. Left: Combined ball-and-stick/polyhedral view representative for $[Fe_4(C_2O_4)_4(H_2O)_2(\beta\text{-}XW_9O_{33})_2]^{14-}$ (Ox_4–$Fe_4X_2W_{18}$; X = As^{III}, Sb^{III}, Bi^{III}). Right: Inner coordination sphere of the two "external" Fe centers. Of the three terminal, labile water ligands two have been replaced by a bidentate oxalate ligand. The three remaining oxygen atoms link to the tungsten-oxo fragment of the POM.

The voltammetric analysis of Ox_4-$Fe_4X_2W_{18}$ (X = As^{III}, Sb^{III}) in aqueous media shows a reduction of the Fe^{III} centers with a 100 mV negative peak potential shift compared to the parent $Fe_4X_2W_{18}$.[18] This is expected, considering the significant increase in negative charge upon oxalate binding. Importantly, the reduction of Ox_4-$Fe_4Sb_2W_{18}$ (two closely spaced waves at −0.280 V and −0.424 V vs SCE, pH 5) occurs at a less negative potential with respect to the As analogous Ox_4-$Fe_4As_2W_{18}$ (a single composite four-electron wave at −0.456 V vs SCE, pH 5), in line with the spectroscopic results discussed above (Figure S18).

The ensemble of structural/spectroscopic/redox evidence allows us to establish a reactivity scenario with a valuable potential in the aerobic oxidation of catechols. Oxidation of DTBC by $Fe_4X_2W_{18}$ (X = As^{III}, Sb^{III}, Se^{IV}, Te^{IV}) has been examined in DCE at 1 atm O_2 pressure and 60 °C. Under the condition explored, 80–90 % substrate conversion occurs in 3 h (entries 1–5 in Table 2). In all cases, the two-electron oxidation product 3,5-di-*tert*-butyl-1,2-benzoquinone (**1**) is formed in 50–60 % yield, along with a mixture of polymeric tars.

Such product distribution indicates that the autoxidation pathway dominates over an almost silent cleavage routine (Scheme 3). Indeed, of the typical intra- or extra-diol cleavage products: 3,5-di-*tert*-butyl-muconic acid anhydride (**2**) or 4,6-di-*tert*-butyl-1-oxacyclohepta-4,6-diene-2,3-dione (**3**) , respectively, the former is detected only in traces (< 2 %).

Table 2. Aerobic oxidation of DTBC catalyzed by $Fe_4X_2W_{18}$.

Entry	Catalyst [mM]	Solvent	Conv. [%]	Cleavage [%][a]	**2**/**3** ratio
1[b]	$Fe_4As_2W_{18}$	DCE	93	< 2	–
2[b]	$Fe_4Sb_2W_{18}$	DCE	91	< 2	–
3[b]	$Fe_4Se_2W_{18}$	DCE	75	< 2	–
4[b]	$Fe_4Te_2W_{18}$	DCE	88	< 2	–
5[c]	$Fe_4As_2W_{18}$	THF/H_2O	95	19	0.2
6[c]	$Fe_4Sb_2W_{18}$	THF/H_2O	91	20	0.28
7[c]	$Fe_4Se_2W_{18}$	THF/H_2O	93	9	0.12
8[c]	$Fe_4Te_2W_{18}$	THF/H_2O	91	31	2.1
9[c,d]	$Fe_4Te_2W_{18}$	THF/H_2O	35	43	6.5

[a] % cleavage selectivity determined by total cleavage products (**2**+**3**)/substrate conversion; [b] reaction performed with catalyst (8.0 mM), 3,5-DTBC (200 mM) at 60 °C for 3 h, $P(O_2)$ = 1 atm, 19–23 turnovers; [c] reaction performed with catalyst (8.0 mM), 3,5-DTBC (60 mM) at 25 °C in THF/H_2O (98:2) in the presence of BHT (0.2 M) for 68 h, $P(O_2)$ = 1 atm, 7 turnovers; [d] reaction performed with 2.5 mM catalyst in the presence of 1 M BHT, 8 turnovers.

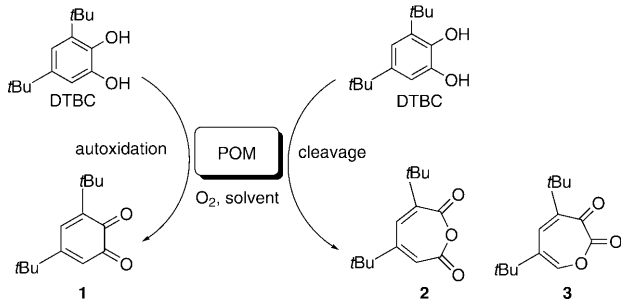

Scheme 3. Competing autoxidation and cleavage pathways in the aerobic oxidation of DTBC catalyzed by $Fe_4X_2W_{18}$.

In an attempt to improve the cleavage selectivity, catalysis has also been explored in other media.[30] The autoxidation process turns out to be faster in CH_3CN and DCE, while it is sensibly slowed down in acetone or in wet THF, in agreement with previous evidence (Figure S21).[31]

Adding to these observations, we also investigated the oxidative screening in wet THF and in the presence of 2,6-di-*tert*-butylcresol (BHT), as radical scavenger to inhibit free-radical oxidation and polymerization pathways (entries 5–9 in Table 2). Indeed, a favorable quinone abatement (< 6 %) and a parallel enhancement of the cleavage selectivity up to > 40 % is obtained (entry 9 in Table 2). In all cases, catalytic cleavage occurs yielding both products **2** and **3**, deriving from an intra- and extra-diol cleavage mechanism, respectively.[32] The Krebs-type structures $Fe_4X_2W_{18}$ appear to be ideally suited for catechol cleavage catalysis. Other types of Fe-containing POMs such as the Keggin derivatives $[Fe(H_2O)(\alpha\text{-}SiW_{11}O_{39})]^{5-}$ and $[\gamma\text{-}Fe_2(H_2O)_2SiW_{10}O_{38}]^{6-}$ are inactive, although they coordinate DTBC (Figures S2, S3, S8, S9). This result is consistent with the key requirements of iron-mediated cleavage of catechols (Scheme 1). Only the Krebs-type POMs feature external Fe centers easily accessible for both catechol and dioxygen binding, thus allowing a possible mechanistic pathway along bio-inspired guidelines.[33] The isostructural Krebs-type catalysts $Fe_4X_2W_{18}$ offer the unique opportunity to correlate the exhibited

cleavage selectivity and the Fe-catechol LMCT interaction (see above). Inspection of entries 7–10 in Table 2 shows that the cleavage performance increases in the order $Fe_4Se_2W_{18}$ < $Fe_4As_2W_{18}$ ≈ $Fe_4Sb_2W_{18}$ < $Fe_4Te_2W_{18}$ indicating that the hetero atom type is crucial. The reactivity trend for DTBC cleavage selectivity of the $Fe_4X_2W_{18}$ catalysts is inversely proportional to their LMCT transition energies in THF/H_2O (Table 1 and Figure 3). Therefore, on the basis of earlier arguments, we associate the increased cleavage specificity to an increase of the Fe Lewis acidity within the $Fe_4X_2W_{18}$ series, by enhancing the semiquinone character of the reactive intermediate and, in a second step, by facilitating the decomposition of the peroxy intermediate to the cleavage products (Scheme 1), in agreement with the enzymatic paradigm.[34]

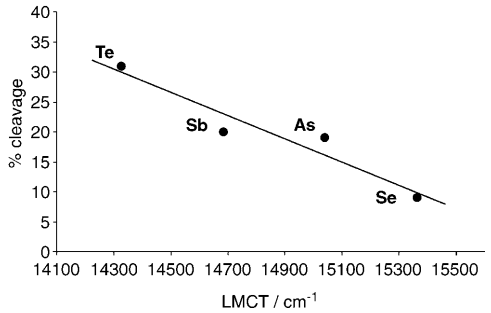

Figure 3. DTBC cleavage selectivity of $Fe_4X_2W_{18}$ catalysts as a function of their LMCT energies in THF/H_2O 98:2 (see also Table 2).

The reactivity correlation traced within the $Fe_4X_2W_{18}$ Krebs-type family provides convincing evidence of the POM involvement, and at the same time, it establishes a fundamental reference point to bridge the gap with classical organic ligands. In this respect, the combined spectroscopic and reactivity evidence is instrumental for a descriptor-aided design of novel dioxygenase functional models, built from totally inorganic POM-based ligands.[35]

Experimental Section

See the Supporting Information for a detailed description of POM synthesis, cation metathesis, XRD details, UV/Vis spectra, electrochemistry and kinetic profiles of oxidation reactions.

Acknowledgements

We thank Ciprian Padurariu for assistance in polyanion synthesis and Francesco Vivan for preliminary catalytic experiments. Financial support from CNR, MIUR (FIRB CAMERE-RBNE03 JCR5), and the ESF COST D40 action are gratefully acknowledged. UK thanks Jacobs University and the Fonds der Chemischen Industrie for research support.

Keywords: catechol cleavage · homogeneous catalysis · iron · polyoxometalates · synzymes

[1] J. S. Valentine, C. S. Foote, A. Greenberg, J. F. Liebman in *Active Oxygen in Biochemistry*, St. Edmundsbury, London, **1995**.
[2] T. Punniyamurthy, S. Velusamy, J. Iqbal, *Chem. Rev.* **2005**, *105*, 2329–2364.
[3] R. Breslow, *Acc. Chem. Res.* **1995**, *28*, 146–153.
[4] B. J. Wallar, J. D. Lipscomb, *Chem. Rev.* **1996**, *96*, 2625–2658.
[5] Special Issue "Polyoxometalates": *Chem. Rev.* **1998**, *98*, 1–387, edited by C. L. Hill.
[6] M. T. Pope, A. Müller in *Polyoxometalate Chemistry: From Topology via Self-assembly to Applications*, Kluwer, Dordrecht, **2002**.
[7] C. L. Hill, C. M. Prosser-McCharta, *Coord. Chem. Rev.* **1995**, *143*, 407–455.
[8] a) M. Costas, M. P. Mehn, M. P. Jensen, L. Que, Jr., *Chem. Rev.* **2004**, *104*, 939–986; b) P. C. A. Bruijnincx, G. van Koten, R. J. M. Klein Gebbink, *Chem. Soc. Rev.* **2008**, *37*, 2716–2744.
[9] T. J. McMurry, J. T. Groves in *Metalloporphyrin Models for Cytochrome P-450* (Ed.: P. R. Ortiz de Montellano), Plenum Press, New York, **1986**.
[10] a) D. K. Lyon, W. K. Miller, T. Novet, P. J. Domaille, E. Evitt, D. C. Johnson, R. G. Finke, *J. Am. Chem. Soc.* **1991**, *113*, 7209–7221; b) D. Mansuy, J. F. Bartoli, P. Battioni, D. K. Lyon, R. G. Finke, *J. Am. Chem. Soc.* **1991**, *113*, 7222–7226.
[11] Y. Nishiyama, Y. Nakagawa, N. Mizuno, *Angew. Chem.* **2001**, *113*, 3751–3753; *Angew. Chem. Int. Ed.* **2001**, *40*, 3639–3641.
[12] S. Shaik, H. Hirao, D. Kumar, *Acc. Chem. Res.* **2007**, *40*, 532–542.
[13] a) D. Kumar, E. Derat, A. M. Khenkin, R. Neumann, S. Shaik, *J. Am. Chem. Soc.* **2005**, *127*, 17712–17718; b) E. Derat, D. Kumar, R. Neumann, S. Shaik, *Inorg. Chem.* **2006**, *45*, 8655–8663; c) D. Barats, G. Leitus, R. Popovitz-Biro, L. J. W. Shimon, R. Neumann, *Angew. Chem.* **2008**, *120*, 10056–10060; *Angew. Chem. Int. Ed.* **2008**, *47*, 9908–9912.
[14] a) A. Sartorel, M. Carraro, G. Scorrano, R. De Zorzi, S. Geremia, N. D. McDaniel, S. Bernhard, M. Bonchio, *J. Am. Chem. Soc.* **2008**, *130*, 5006; b) G. Süss-Fink, *Angew. Chem.* **2008**, *120*, 5972–5974; *Angew. Chem. Int. Ed.* **2008**, *47*, 5888–5890.
[15] C. X. Yin, R. G. Finke, *Inorg. Chem.* **2005**, *44*, 4175–4188.
[16] a) B. Botar, Y. V. Geletii, P. Kögerler, D. G. Musaev, K. Morokuma, I. A. Weinstock, C. L. Hill, *J. Am. Chem. Soc.* **2006**, *128*, 11268–11277; b) M. Bonchio, M. Carraro, A. Farinazzo, A. Sartorel, G. Scorrano, U. Kortz, *J. Mol. Catal. A* **2007**, *262*, 36–40.
[17] M. Bonchio, M. Carraro, A. Sartorel, G. Scorrano, U. Kortz, *J. Mol. Catal. A* **2006**, *251*, 93–99.
[18] U. Kortz, M. G. Savelieff, B. S. Bassil, B. Keita, L. Nadjo, *Inorg. Chem.* **2002**, *41*, 783–789.
[19] a) H. Weiner, Y. Hayashi, R. G. Finke, *Inorg. Chim. Acta* **1999**, *291*, 426–437; b) H. Weiner, R. G. Finke, *J. Am. Chem. Soc.* **1999**, *121*, 9831–9842 and references therein; c) C. X. Yin, R. G. Finke, *J. Am. Chem. Soc.* **2005**, *127*, 9003–9013.
[20] a) *Oxygenases and Model Systems* (Ed.: T. Funabiki), Kluwer, Dordrecht, **1997**; b) L. Que, Jr., R. Y. N. Ho, *Chem. Rev.* **1996**, *96*, 2607–2624.
[21] a) H.-J. Krüger in *Biomimetic Oxidations Catalyzed by Metal Complexes* (Ed.: B. Meunier), Imperial College Press, London, **2000**; b) P. E. M. Siegbahn, T. Borowski, *Acc. Chem. Res.* **2006**, *39*, 729–738; c) P. C. A. Bruijnincx, M. Lutz, A. L. Spek, W. R. Hagen, B. M. Weckhuysen, G. van Koten, R. J. M. Klein Gebbink, *J. Am. Chem. Soc.* **2007**, *129*, 2275–2286; d) P. C. A. Bruijnincx, M. Lutz, A. L. Spek, W. R. Hagen, G. van Koten, R. J. M. Klein Gebbink, *Inorg. Chem.* **2007**, *46*, 8391–8402.
[22] H. G. Jang, D. D. Cox, L. Que, Jr., *J. Am. Chem. Soc.* **1991**, *113*, 9200–9204.
[23] D. D. Cox, S. J. Benkovic, L. M. Bloom, F. C. Bradley, M. J. Nelson, L. Que Jr. , D. E. Wallick, *J. Am. Chem. Soc.* **1988**, *110*, 2026–2032.

[24] The stability of the polyanions upon DTBC addition or adventitious H_2O_2 was confirmed by FT-IR (see the Supporting Information). The same complexes have been found highly robust under harsher autoxidation conditions with microwave assisted protocols see M. Bonchio, M. Carraro, G. Scorrano, U. Kortz, *Adv. Synth. Catal.* **2005**, *347*, 1909–1912.
[25] A blue-shift of the λ_{max} values is observed upon coordination of less electron donating catechols due to less favorable LMCT transitions: indeed λ_{max} values of $Fe_4Te_2W_{18}$ upon addition of 4-*tert*-butylcatechol and 4-chlorocatechol in DCE are at 729 nm (shoulder at 652) and 671 nm (shoulder at 622 nm), respectively.
[26] D. D. Cox, L. Que, Jr., *J. Am. Chem. Soc.* **1988**, *110*, 8085–8092.
[27] a) M. Pascaly, M. Duda, F. Schweppe, K. Zurlinden, F. K. Muller, B. Krebs, *J. Chem. Soc. Dalton Trans.* **2001**, 828–837; b) P. Mialane, L. Tchertanov, F. Banse, J. Sainton, J.-J. Girerd, *Inorg. Chem.* **2000**, *39*, 2440–2444.
[28] Synthesis and crystal data of Ox_4-$Fe_4X_2W_{18}$ are reported in the Supporting Information. CCDC 724754, 724755, and 724756 contain the supplementary crystallographic data for this paper. These data can be obtained free of charge from The Cambridge Crystallographic Data Centre via www.ccdc.cam.ac.uk/data_request/cif.
[29] A. Dolbecq, J.-D. Compain, P. Mialane, J. Marrot, E. Rivière, F. Sécheresse, *Inorg. Chem.* **2008**, *47*, 3371–3378.
[30] Reactivity screening has also been extended in the following solvents: DMF, CH_3CN, acetone, chlorobenzene, toluene, and in mixed media: CH_3CN/pyridine 1:8, THF/CH_3CN 1:2, DCE/*tert*-butanol 1:1, CH_3CN/*tert*-butanol 1:1, as well as the non-conventional supercritical CO_2. These experiments have been performed with $Fe_4As_2W_{18}$, isolated as a THA, TBA or PPh_4 salt by cation metathesis, which offers an optimal synthetic strategy for tuning the solubility of the POM catalyst (Table S5 in the Supporting Information).
[31] THF/H_2O 98:2 was reported to be an effective solvent for this reaction, see: T. Funabiki, I. Yoneda, M. Ishikawa, M. Ujiie, Y. Nagai, S. Yoshida, *J. Chem. Soc. Chem. Commun.* **1994**, 1453.
[32] GC-MS and ^{1}H NMR exclude the formation of five-member ring 2-pyrones. A non-regioselective cleavage is generally observed in abiotic systems. Computational arguments point at a subtle interplay of factors that might modulate the oxidative cleavage preference. See reference [21].
[33] Control experiments with iron-free derivatives allow to establish that the observed reactivity is ascribable to the POM embedded iron centers Specifically, isostructural complexes of the type $[\beta\text{-}M_4(H_2O)_{10}(XW_9O_{33})_2]^{n-}$ where M is Cr^{III}, Mn^{II}, Co^{II}, Ni^{II}, Cu^{II}, and Cd^{II} lead to negligible DTBC conversion ($<2\%$).
[34] L. Que, Jr., R. C. Kolanczyk, L. S. White, *J. Am. Chem. Soc.* **1987**, *109*, 5373–5380.
[35] The pioneering work on transition-metal supported POMs is inspiring as this POM structural type displays *cis*-coordination sites, coordinative unsaturation, interesting reactivity and selectivity, see reference [19a] and H. Weiner, Y. Hayashi, R. G. Finke, *Inorg. Chem.* **1999**, *38*, 2579–2591.

Received: May 25, 2009
Published online: July 8, 2009

